Atmos. Chem. Phys. Discuss., 7, 9867–9897, 2007
www.atmos-chem-phys-discuss.net/7/9867/2007/

Atmospheric Chemistry and Physics Discussions

The Response of surface ozone to climate change over the Eastern United States

P. N. Racherla[1] **and P. J. Adams**[2]

[1]Dept. of Engineering and Public Policy, Carnegie Mellon University, Pittsburgh, PA, USA
[2]Dept. of Civil and Environmental Engineering and Engineering and Public Policy, Carnegie Mellon University, Pittsburgh, PA, USA

Received: 18 June 2007 – Accepted: 2 July 2007 – Published: 9 July 2007

Correspondence to: P. N. Racherla (pavanracherla@cmu.edu)

Abstract

We examined the response of surface ozone to future climate change over the eastern United States by performing simulations corresponding to present (1990s) and future (2050s) climates using an integrated model of global climate, tropospheric gas-phase chemistry, and aerosols. A future climate has been imposed using ocean boundary conditions corresponding to the IPCC SRES A2 scenario for the 2050 s decade, resulting in an increase in the global annual-average surface air temperature by 1.7°C, with a 1.4°C increase over the surface layer of the eastern United States. Present-day anthropogenic emissions and CO_2/CH_4 mixing ratios have been used in both simulations while climate-sensitive natural emissions were allowed to vary with the simulated climate. There is practically zero change in the spatiotemporally averaged ozone mixing ratios predicted over the eastern United States. However, the severity and frequency of ozone episodes over the eastern United States increased due to future climate change, primarily as a result of increased ozone chemical production due to increased natural isoprene emissions. The 95th percentile ozone mixing ratio increased by 5 ppbv and the largest frequency increase occured in the 80–90 ppbv range. The most substantial and statistically significant (p-value <0.05) increases in episode frequency occurred over the southeast and midatlantic United States, largely as a result of 20% higher annual-average natural isoprene emissions. Increased chemical production and shorter average lifetime are consistent features of the predicted seasonal surface ozone response, with the former's magnitude for a location largely a function of increased natural isoprene emissions, and the latter largely due to faster dry deposition removal rates. Future climate change is also predicted to lengthen the ozone season over the eastern United States to include late spring and early fall. Significant interannual variability is observed in the frequency of ozone episodes and we find that it is necessary to utilize 5 years or more of simulation data in order to separate the effects of interannual variability and climate change on ozone episodes.

ACPD

7, 9867–9897, 2007

1 Introduction

The reduction of surface ozone, which is harmful to human, animal, and plant health, is an important objective of air quality policy for many governments. Surface ozone is produced through a complex set of photochemical reactions involving NO_x (= NO+NO_2) and volatile organic compounds (VOCs). NO_x and VOCs are emitted from anthropogenic sources such as fossil fuel power plants, industrial activities and transportation, as well as natural sources such as lightning and soil (NO_x), and vegetation (biogenic VOCs such as isoprene). The resulting ozone concentrations depend sensitively upon meterological parameters such as temperature, cloudiness, sunlight, wind speeds and the mixed layer depth. Therefore, changes in these meteorological parameters due to climate change will necessarily impact surface ozone concentrations. However, the direction of change itself is often unclear because of multiple competing effects.

A major conclusion of many previous global modeling studies (Brasseur et al., 1998; Stevenson et al., 2000; Zeng and Pyle, 2003; Liao et al., 2006; Racherla and Adams, 2006), which have assessed the effect of future climate change on global tropospheric ozone is that the global average burden of ozone decreases because of the increased destruction of ozone due to increased water vapor concentrations. In these studies, although ozone chemical production increases it is dominated by the increased destruction of ozone on a global scale in the absence of changes in emissions. On the other hand, Collins et al. (2003); Zeng and Pyle (2003) suggest that the stratosphere-troposphere exchange of ozone is likely to increase due to climate change, which increases tropospheric ozone. Hauglustaine et al. (2005) predict an increase in the upper tropospheric ozone concentrations due to climate change, which is primarily due to increased lightning NO_x caused by more intense convective activity.

While a number of previous modeling studies (Sillman and Samson, 1995; Aw and Kleeman, 2003; Baertsch-Ritter et al., 2004; Dawson et al., 2007) have focused on the effect of individual meteorological parameters on surface ozone, only a few studies have assessed holistically the effect of future climate change. One major conclusion

of the former kind of modeling studies is that ozone increases with temperature in both urban and polluted rural environments, with the increase driven largely by a decrease in the formation of peroxyacetyl nitrate (PAN), thereby increasing NO_x concentrations. Hogrefe et al. (2004) used a regional air quality model centered over the eastern United States to evaluate climate change impacts on air quality and found that increases of up to 5 ppbv are likely in the summertime average daily maximum 8-h ozone concentrations by the 2080s. Murazaki and Hess (2006) used a global chemical transport model model (CTM) driven by future meteorology and present-day emissions (IPCC SRES A1 scenario 2090 s) and found that the increased NO_x concentrations, resulting from reduced PAN in a warmer climate, predominantly affected surface ozone production in polluted regions. This is because increased water vapor concentrations, as a result of climate change, are expected to increase net ozone production in regions with high NO_x through the reaction $NO+HO_2 \rightarrow NO_2+OH$, but to decrease net ozone production in regions with low NO_x through the competing ozone sink $O_3+HO_2 \rightarrow 2O_2+OH$. Hauglustaine et al. (2005) and Liao et al. (2006) emphasize the potentially important effect of increased biogenic VOC emissions due to future climate change (IPCC SRES A2 scenario 2090s) on surface ozone levels; based on their sensitivity studies, performed with a global model, they report that increased natural isoprene emissions account for 30–50% of the predicted increases in future surface ozone levels over polluted regions such as the eastern United States, western Europe, and northern China.

Only a few modeling studies (Mickley et al., 2004; Hogrefe et al., 2004; Murazaki and Hess, 2006) have examined the effect of future climate change on regional air pollution. A feature of climate change that emerges from these studies is a decrease in the frequency and intensity of synoptic frontal passages ventilating the boundary layer over the United States. The effect of these changes on future surface ozone levels is not very well understood, however, as it is complicated by simultaneous changes in other processes such as the precursor chemistry, boundary layer mixing, and convection. Nevertheless, all of the above mentioned modeling studies find an increase in the frequency and severity of future air pollution episodes.

Previous global and regional modeling studies that have examined the response of surface ozone to future climate change at regional scales, although relevant, suffer from one or more of the following limitations: (1) neglect climate change impacts outside their domain due to their assumption of constant boundary conditions (BCs); (2) do not consider the climate-sensitivity of ozone precursor emissions such as isoprene; and, (3) do not examine the seasonality of the ozone response, as they focus on summertime ozone.

The objective of this study is to examine the seasonal and regional response of surface ozone to future climate change, with a focus on the eastern United States. Anthropogenic emissions are held constant between present and future simulations, but the model allows climate-sensitive biogenic emissions to vary with future climate. So as to be useful to near-term energy and air quality policy, we consider a climate change scenario (IPCC SRES A2) corresponding to the 2050s. We examine the effects of climate change on the severity and frequency of ozone episodes, surface layer ozone budget, and the length of the ozone season. We also examine the effect of interannual variability vis-a-vis the predicted impacts due to climate change. Details of the model, the emissions utilized, and the simulations performed are provided in Sect. 2. The results are presented and discussed in Sect. 3. Finally, we present our conclusions in Sect. 4.

2 Methods

2.1 Model overview

We utilize a "unified" global model (Liao et al., 2003, 2004) of climate, photochemistry, and aerosols consisting of: (1) the Goddard Institute for Space Studies general circulation model II' (GISS GCM II') (Hansen et al., 1983; Rind and Lerner, 1996; Rind et al., 1999); (2) the Harvard tropospheric O_3-NO_x-hydrocarbon chemical model (Mickley et al., 1999); and, (3) an aerosol model including sulfate, nitrate, ammonium, black

carbon, and organic carbon (Adams et al., 1999; Chung and Seinfeld, 2002; Liao et al., 2003, 2004).

The version of GISS GCM II' incorporated in the current study is an atmosphere only GCM. It has a horizontal resolution of 4° latitude by 5° longitude, with nine vertical layers centered at 959, 894, 786, 634, 468, 321, 201, 103, and 26 hPa. The model uses specified monthly mean ocean boundary conditions in the form of sea surface temperatures (SSTs), sea-ice coverage and sea-ice mass. The dynamical time step of the GCM is 1 hour. Necessary GCM variables are passed to the tropospheric gas-phase chemistry and aerosol modules every 4 h.

The model transports 88 species; of these, 24 species are used to describe O_3-NO_x-hydrocarbon chemistry; the remainder are for the simulation of the aerosols. The model is constrained in the stratosphere by applying flux upper boundary conditions between the seventh and eighth model layers (approximately 150 hPa) to represent transport across the tropopause (Wang et al., 1998; Mickley et al., 1999). The flux upper boundary conditions for ozone is based on the observed latitudinally and seasonally dependent cross-tropopause air mass fluxes (Appenzeller et al., 1996), along with ozonesonde measurements at 100 hPa (Logan, 1999). In the current study, a stratospheric ozone flux of 400 $Tg\,yr^{-1}$, which was used in the previous model versions (Liao et al., 2003), is specified. We use this value in both present and future climate simulations discussed in Sect. 2.4.

The dry deposition of all gas-phase species is determined based on the resistance-in-series scheme of Wesely (1989), wherein the dry deposition velocity is inversely proportional to the sum of the aerodynamic, quasi-laminar sublayer and surface resistances (Wang et al., 1998). The aerodynamic and quasi-laminar sublayer resistances are calculated based on the GCM surface fluxes of momentum and heat while the surface resistance is a function of the surface type and the species. Wet deposition is coupled with the GCM treatment of clouds and precipitation (Koch et al., 1999; Del Genio and Yao, 1993; Del Genio et al., 1996).

2.2 Isoprene chemistry

Pertinent to this study is the model's isoprene oxidation mechanism, the details of which are provided in Horowitz et al. (1998) and references therein. The primary oxidation pathways for isoprene are the reactions with OH, O_3, and NO_3. The reaction with OH is the dominant sink, and it produces a variety of peroxy radicals (lumped together as RIO_2). The principal branch of the NO+RIO_2 reaction produces HO_2, methacrolein, methylvinyl ketone, formaldehyde, and other carbonyl compounds. Of particular importance is the model's treatment of the secondary branch of NO+RIO_2, which produces isoprene nitrates, with an assumed yield of 12%. The model assumes that the isoprene nitrates react rapidly with OH and O_3 and return NO_x to the atmosphere with 100% efficiency.

The model's assumption of 100% recycling of isoprene nitrates to NO_x is quite uncertain as some field studies have suggested that the isoprene nitrates are likely to deposit quickly, i.e., on a timescale comparable to HNO_3 deposition, thereby removing NO_x from the atmosphere (Giacopelli et al., 2005). However, a more recent modeling-observational analysis by Horowitz et al. (2007) suggests that atmospheric observations of total organic nitrates were best supported when an isoprene nitrate yield of 4 to 8% and 40% recycling of isoprene nitrates to NO_x was assumed. Nevertheless, that analysis did not rule out the possibility of 100% NO_x recycling.

2.3 Emissions

The anthropogenic emissions used in the model are summarized in Liao et al. (2003, 2004). These emissions correspond to the present-day; we utilize them in both the present and future climate simulations discussed in Sect. 2.4. Climate-sensitive ozone precursor emissions include isoprene, biogenic lumped $\geq C_3$ alkenes, biogenic acetone, lightning NO_x, and soil NO_x. The model, however, does not consider the climate-sensitivity of emissions of reactive hydrocarbons with potential for aerosol formation, which include monoterpenes and sesquiterpenes. The model assumes a static vegeta-

tion distribution and corresponding base isoprene emissions from the Global Emission Inventory Activity (GEIA) (Guenther et al., 1995). The isoprene emitted in a model grid cell and a time step is a function of the leaf area, and the GCM provided 4-hourly values of temperature and solar radiation (Guenther et al., 1995; Wang et al., 1998). Biogenic emissions of lumped $\geq C_3$ alkenes and acetone are estimated by scaling to isoprene emissions (Goldstein et al., 1996; Singh et al., 1994). The emission ratios per atom C isoprene are 0.051 atoms C for lumped $\geq C_3$ alkenes and 0.015 molecules for acetone. The parameterizations for lightning NO_x and soil NO_x emissions are provided in Wang et al. (1998); the meteorological parameters that influence their emissions are the frequency of convective events, and temperature and precipitation, respectively. Therefore, the model treats the climate sensitivity of these emissions such that the emissions rates of these species change between the present and future climate simulations discussed in Sect. 2.4.

2.4 Simulations

Two simulations, each of ten and a half years duration, were performed with the first six months ignored to allow for model initialization. The first simulation corresponds to present climate (1990s) while the second simulation corresponds to a future climate (IPCC SRES A2 scenario 2050s). Hereafter, we refer to these simulations as present and future climate simulations, and abbreviate them as PC simulation and FC simulation, respectively. Present-day anthropogenic emissions were used in both the runs while natural climate-sensitive emissions were allowed to vary with the simulated climate (see Sect. 2.3). For the analyses that follow, we use 4-h average surface ozone mixing ratios, 10 simulation years worth, saved over the eastern United States (105–65° W and 24–48° N), corresponding to 38 model cells in total (pure ocean cells are excluded). For the surface-layer ozone budgets, however, we utilize monthly-average values.

A present-day CO_2 mixing ratio of 370 ppmv and 1.7 ppmv for CH_4 was specified in both simulations. Future climate is imposed by changing the ocean boundary condi-

tions that drive the GCM. This alternate approach to simulating climate change is attractive because it avoids the large amounts of computer time that would be required to simulate the dynamics and transient response of the ocean, if a greenhouse gas forcing were imposed on the system (Cess et al., 1990). The ocean boundary conditions used in this study are obtained from separate transient climate simulations performed using a fully coupled atmosphere-ocean GCM (the GISS Model III, Russell et al., 1995, personal communication with R. Healy), with greenhouse gas radiative forcings from the IPCC SRES A2 scenario. Details of these transient climate simulations are provided in Robertson et al. (2001). We use the decadally averaged ocean boundary conditions (1990s/2050s) from the above transient climate simulation, with month-to-month variability.

The predicted climate change corresponds to an increase in the global annual-average surface air temperature by 1.7°C, with a 1.4°C increase over the surface layer of the eastern United States (see Table 1). While these changes are useful for understanding average surface ozone changes, they are limited when it comes to the analysis of changes in air pollution episodes, which will require more time-resolved values of related meteorological parameters.

3 Results

3.1 Severity and frequency of ozone episodes

Figure 1 shows box-and-whisker plots of the predicted surface ozone mixing ratios for the PC and FC simulations. These data are not spatially averaged. The model predicts practically zero change in the spatiotemporally averaged ozone mixing ratios, as can be seen from the nearly identical surface ozone median values for the PC and FC simulations. The most noticeable difference between the PC and FC simulation surface ozone distributions, however, is in the upper extreme, wherein the model predicts a 5 ppbv increase in the 95th percentile value for the FC simulation. We conclude that

the severity of high-ozone events increases in the FC simulation.

The difference between the PC and FC simulations surface ozone distributions is emphasized in Fig. 2, which shows truncated surface ozone probability distribution functions (PDFs) for the two simulations. The model predicts an increased probability of high-ozone events in the FC simulation, with the largest increase occurring in the 80–90 ppbv range. Hereafter, we refer to high-ozone events as ozone "episodes", which we define as any occurrence, in a model grid cell, of a 4-h average surface ozone mixing ratio greater than 80 ppbv (the United States Environmental Protection Agency's (US EPA) 8-h primary standard for surface ozone). These results lead us to the conclusion that the frequency of ozone episodes increases in the FC simulation.

Figure 3a shows the spatial distribution of the predicted yearly frequencies (10-year average) of ozone episodes over the eastern United States in the base case (PC simulation) while Figure 3b shows the differences (FC simulation minus PC simulation) in the yearly frequencies of ozone episodes. The model predicts an increased frequency of ozone episodes over most of the eastern United States, with substantial increases of 30-50 episodes per year over some southeast and midatlantic states. We confirmed that these substantial increases over the southeast and midatlantic United States are also statistically significant (p-value <0.05) by performing a Student's t test upon the 10-year distributions of the yearly frequency of ozone episodes in those model grid cells for the PC and FC simulations. Collectively, these results show that the severity and frequency of ozone episodes over the eastern United States increases due to climate change, with substantial and statistically significant increases occurring over the southeast and midatlantic states.

Previous modeling studies by Mickley et al. (2004) and Murazaki and Hess (2006) suggest that the severity of future summertime air pollution episodes in the northeastern and midwestern United States will increase due to reduced cyclone frequency in a warmer climate. We examined the 4-hour average sea level pressure (SLP) anomaly distributions over several model grid cells in the eastern United States to investigate whether circulation changes (e.g. reduced cyclone frequency) play a role in the pre-

dicted increases in our FC simulation (see Fig. 4). The model predicts up to a 4% difference in the cumulative probabilities at the low-end (decrease) and the high-end (increase). Using a Kolmogorov-Smirnov test, we found that these changes are far from significant, however, as the p-values are much greater than 0.05.

It is possible that the above changes correspond to a reduction in cyclones and an increase in stagnation events, respectively, and are enough to have contributed somewhat to the predicted changes. Regardless, our analysis (see Sect. 3.2) shows that the changes in O_3 chemical production play the dominant role in the southeast and midatlantic United States, where the most substantial increases in ozone episodes occur in the FC simulation. In contrast to the cited earlier work, we do not find unambiguous evidence of circulation changes driving the increase in ozone episodes. Some possible reasons for this apparent discrepancy with previous studies are: a) the different SSTs that we utilize; and, b) the different methodology that we have employed to detect circulation changes, i.e., SLP anomaly distributions as opposed to a cyclone tracking method (Mickley et al., 2004).

3.2 The seasonal response of surface ozone

Table 2 shows the seasonal surface-layer odd oxygen (O_x) budgets over the southeast and midatlantic United States for the PC and FC simulations (10 year average). For the purpose of this budget, O_x is defined as the sum of ozone, O, NO_2, 2 x NO_3, 3 x N_2O_5, HNO_4, HNO_3, and the peroxyacylnitrates. We present the O_x budget for the southeast and midatlantic United States in order to illustrate the factors that contribute to the substantial increases in the severity and frequency of ozone episodes for that region in the FC simulation. It can be seen from Table 2 that two consistent features of the seasonal surface ozone response to climate change are the increased ozone chemical production and shorter average ozone lifetime.

Table 3 provides a summary of a number of factors controlling ozone chemical production over the southeast and midatlantic United States. The increased ozone chemical production is largely due to higher natural isoprene emissions. Increased isoprene

levels result in higher peroxy radical (RO_2 and HO_2) concentrations, which, in turn, result in increased net ozone chemical production through $NO+RO_2$ and $NO+HO_2$. We estimated the impact of increased natural isoprene emissions on ozone episodes over the eastern United States (see Fig. 5) by performing a simulation (5 consecutive summers) with future meteorology, wherein the model evaluated isoprene emissions were scaled down uniformly by a factor of 1.2, globally. That factor corresponds to the 10-year average of the ratio of isoprene emissions in the FC to the PC simulations over the eastern United States. It is evident from Fig. 5 that in the FC simulation 50–60% of the increase in summertime ozone episodes over the southeast and midatlantic United States is due to increased natural isoprene emissions. The remainder of the increase in ozone episodes in the FC simulation is most likely due to the ozone-temperature relationship (Jacob et al., 1993). We conclude from these results that in the FC simulation the increased ozone chemical production, largely due to increased natural isoprene emissions, is responsible for up to 60% of the increase in ozone episodes over the southeast and midatlantic United States.

Although the annual-average PAN mixing ratio over the southeast and midatlantic United States decreased by 9% in our FC simulation, it does not result in a corresponding increase in the NO_x mixing ratio, which, in fact decreased by 1%. That decrease in the NO_x mixing ratio occurs because of the increased peroxy radical concentrations due to increased isoprene emissions, which results in a reduced $NO:NO_2$ ratio by 10%. As a result, more NO_x is present as NO_2, where it is more likely to undergo oxidation to NO_y. The constant-isoprene sensitivity simulation mentioned earlier adds strength to that argument because the NO_x mixing ratio increased by nearly 6% when future isoprene emissions were reduced to their present-day levels.

Even in the absence of vegetation changes, future changes in biogenic VOC emissions could occur due to changes in the meteorological parameters that influence them. For example, in the FC simulation, over the southeast and midatlantic United States, warmer temperatures and reduced cloud cover contributed to increased isoprene emissions. By contrast, we found that over the Mediterranean the cloud cover increased,

resulting in a slight reduction in the isoprene emissions. These predicted changes in future biogenic VOC emissions (eg. isoprene) over specific geographical regions must be regarded as somewhat uncertain, however, given the uncertainty in cloud processes in global climate models (Cess et al., 1990).

The shorter surface ozone lifetime during all seasons in the FC simulation is primarily due to increased dry deposition removal rates and to some extent the increased total chemical loss rates. The increased dry deposition removal rate is due to reduced aerodynamic and quasi-laminar sublayer resistance, as a result of increased wind speeds. The change in the surface resistance itself plays a negligible role because key surface parameters such as the leaf area index are being held constant between the PC and FC simulations. The increased total chemical loss rate is due to increased HO_x and RO_x concentrations resulting from the increased isoprene emissions.

Figure 6 shows the probability of an ozone episode occurring over the eastern United States during any 4-h period for the PC and FC simulations, January through December. We utilize the changes in ozone episode probability as a surrogate for the changes in length of the ozone season. As expected, for both the PC and FC simulations, the summer months (June through August) display the highest probability for the occurrence of ozone episodes. While the largest absolute increases occur predominantly in the summer months, it is interesting to note the larger relative increases in episode probability in the FC simulation during the fall (September/October) and spring (April/May) seasons, which, generally, have very few ozone episodes under present-day meteorology and emissions. Collectively, these findings suggest a lengthening of the ozone season over the eastern United States to include late spring and early fall months.

3.3 The effect of interannual variability

Our modeling shows that with only a few years (e.g. 2 years) of simulation data, it is difficult to separate the effects of interannual variability and climate change on ozone episodes. This is illustrated in Table 4, wherein we show the ratio of the mean difference

(FC simulation minus PC simulation) in the annual frequency of ozone episodes to the standard error for the same, given 1, 5, and 10 years worth simulation results for 5 model grid cells in the southeast and midatlantic United States. That ratio allows us to examine the statistical significance of the climate change (signal) to interannual variability (noise) vis-a-vis the predicted changes. It is evident from Table 4 that after 1 year 30–46% of the difference could be attributed to interannual variability alone and it drops to 14–20% for 5 years; after 5 years the ratio remains fairly constant. We conclude from these results that it is necessary to utilize 5 years or more of simulation data in order to separate the effects of future climate change and interannual variability on ozone episodes.

4 Conclusions

We have investigated the response of surface ozone to climate change over the eastern United States by performing simulations corresponding to present (1990s) and future (2050s) climates using an integrated model of global climate, tropospheric gas-phase chemistry, and aerosols. Future climate is imposed using ocean boundary conditions corresponding to the IPCC SRES A2 scenario for the 2050s decade. The predicted climate change corresponds to an increase in the global annual-average surface air temperature by 1.7°C, with a 1.4°C increase over the surface layer of the eastern United States. Present-day anthropogenic emissions and CO_2/CH_4 mixing ratios were used in both simulations while climate-sensitive natural emissions were allowed to vary with the simulated climate.

Our results show that the severity and frequency of ozone episodes over the eastern United States increases due to future climate change, primarily as a result of increased surface ozone chemical production. The 95th percentile ozone mixing ratio increases by 5 ppbv and the largest increase in the frequency occurs in the 80–90 ppbv range. The most substantial and statistically significant (p-value <0.05) increases in episode frequency occur over the southeast and midatlantic United States, largely as a result

of 20% higher annual average natural isoprene emissions. We also examined the extent to which circulation changes influenced the increased severity and frequency of ozone episodes by comparing the sea level pressure distributions over several model grid cells for the present and future climate simulations. That analysis did not provide conclusive evidence pointing to systematic circulation changes and their role in the increased frequency of ozone episodes.

These results suggest a lengthening of the ozone season over the eastern United States to include late spring and early fall months, with increased chemical production and shorter average ozone lifetime in the FC simulation being two consistent features of the predicted seasonal response of surface ozone. Our analysis shows that the magnitude of the increased ozone chemical production for a region is largely dependent on the increase in natural isoprene emissions, which is largest over the southeast and midatlantic United States. The shorter surface ozone lifetime over the eastern United States is primarily due to increased dry deposition removal rates, and to a lesser extent, the increased chemical loss rates.

Our modeling suggests that changes in natural isoprene emissions may have a significant effect on surface ozone levels over regions such as the southeast and midatlantic United States, where it increased as a result of warmer temperatures and reduced cloud cover. Our sensitivity analysis shows that the higher isoprene levels account for 50–60% of the increased summertime ozone episodes in the future climate simulation for that region. The model predicted changes in surface ozone due to isoprene chemistry must be treated as somewhat uncertain, however, given the uncertanties in the future changes of the influencing meteorological factors such as cloud cover, as well as uncertainties due to the base isoprene emissions inventory used and the fate of isoprene nitrates (Fiore et al., 2005).

These results show that there is significant interannual variability in the frequency of ozone episodes. For example, we found that after 1 year 30–46% of the increase in the yearly frequency of ozone episodes could be attributed to interannual variability alone, which, after 5 years or more of simulation data, drops to 14–20%. We conclude

that it is necessary to utilize 5 years or more of simulation data in order to separate the effects of future climate change and interannual variability on ozone episodes.

Acknowledgements. This work was supported by the NCER STAR Program, EPA (Agreement Number: RD-83096101-0). We would like to thank R. Healy at WHOI for his help.

References

Adams, P. J., Seinfeld, J. H., and Koch, D. M.: Global concentrations of tropospheric sulfate, nitrate, and ammonium aerosol simulated in a general circulation model, J. Geophys. Res., 104, 13 791–13 823, 1999. 9872

Appenzeller, C., Holton, J. R., and Rosenlof, K. H.: Seasonal variation of mass transport across the tropopause, J. Geophys. res., 101, 15 071–15 078, 1996. 9872

Aw, J. and Kleeman, M. J.: Evaluating the first-order effect of intraannual temperature variability on urban air pollution, J. Geophys. Res., 108, 4365, doi:10.1029/2002JD002688, 2003. 9869

Baertsch-Ritter, N., Keller, J., Dommen, J., and Prevot, A. S. H.: Effects of various meteorological conditions and spatial emission resolutions on the ozone concentration and ROG/NO_x limitation in the Milan area (I), Atmos. Chem. Phy., 4, 423–438, 2004. 9869

Brasseur, G., Kiehl, J., Schneider, T., Granier, C., Tie, X., and Hauglustaine, D.: Past and future changes in global tropospheric ozone: Impact on radiative forcing, Geophys. Res. Lett., 25, 3807–3810, 1998. 9869

Cess, R. D. et al.: Intercomparison and interpretation of climate feedback processes in 19 atmospheric general-circulation models, J. Geophys. Res., 95, 16 601–16 615, 1990. 9875, 9879

Chung, S. H. and Seinfeld, J. H.: Global distribution and climate forcing of carbonaceous aerosols, J. Geophys. Res., 107, 4407, 2002. 9872

Collins, W. J., Derwent, R. G., Garnier, B., Johnson, C. E., Sanderson, M. G., and Stevenson, D. S.: Effect of stratosphere-troposphere exchange on the future tropospheric ozone trend, J. Geophys. Res., 108, 8528, doi:10.1029/2002JD002617, 2003. 9869

Dawson, J. P., Adams, P. J., and Pandis, S. N.: Sensitivity of ozone to summertime climate in the eastern USA: A modeling case study, Atmos. Environ., 41, 1494–1511, 2007. 9869

Del Genio, A. D. and Yao, M. S.: Efficient cumulus parameterization for long-term climate studies: The GISS scheme, in: The Representation of Cumulus Convection in Numerical Models,

Monogr. 46, edited by: Emanuel, K. A. and, Raymond D. J., 181–184, Am. Meteorol. Soc., Boston, Mass., 1993., 1993. 9872
Del Genio, A. D., Yao, M. S., Kovari, W., and Lo, K. K. W.: A prognostic cloud water parameterization for global climate models, J. Clim., 9, 270–304, 1996. 9872
Fiore, A. M., Horowitz, L. W., Purves, D. W., Levy, H., Evans, M. J., Wang, Y. X., Li, Q. B., and Yantosca, R. M.: Evaluating the contribution of changes in isoprene emissions to surface ozone trends over the eastern United States, J. Geophys. Res., 110, D12303, doi:10.1029/2004JD005485, 2005. 9881
Giacopelli, P., Ford, K., Espada, C., and Shepson, P.: Comparison of the measured and simulated isoprene nitrate distributions above a forest canopy, J. Geophys. Res., 110, D01304, doi:10.1029/2004JD005123, 2005. 9873
Goldstein, A., Fan, S., Goulden, M., Munger, J., and Wofsy, S.: Emissions of ethene, propene, and 1-butene by a midlatitude forest, J. Geophys. Res., 101, 9149–9158, 1996. 9874
Guenther, A., Hewitt, C., Erickson, D., Fall, R., Geron, C., Graedel, T., Harley, P., Klinger, L., Lerdau, M., McKay, W., et al.: A global model of natural volatile organic compound emissions, J. Geophys. Res, 100, 8873–8892, 1995. 9874
Hansen, J., Russell, G., Rind, D., Stone, P., Lacis, A., Lebedeff, S., Ruedy, R., and Travis, L.: Efficient 3-dimensional global-models for climate studies: MODEL-I and MODEL-II, Mon. Weather Rev., 111, 609–662, 1983. 9871
Hauglustaine, D. A., Lathiere, J., Szopa, S., and Folberth, G. A.: Future tropospheric ozone simulated with a climate-chemistry-biosphere model, Geophys. Res. Lett., 32, L24807, doi:10.1029/2005GL024031, 2005. 9869, 9870
Hogrefe, C., Lynn, B., Civerolo, K., Ku, J. Y., Rosenthal, J., Rosenzweig, C., Goldberg, R., Gaffin, S., Knowlton, K., and Kinney, P. L.: Simulating changes in regional air pollution over the eastern United States due to changes in global and regional climate and emissions, J. Geophys. Res, 109, D22 301, 2004. 9870
Horowitz, L., Liang, J., Gardner, G., and Jacob, D.: Export of reactive nitrogen from North America during summertime- Sensitivity to hydrocarbon chemistry, J. Geophys. Res., 103, 13 451–13 476, 1998. 9873
Horowitz, L., Walters, S., Mauzerall, D., Emmons, L., Rasch, P., Granier, C., Tie, X., Lamarque, J., Schultz, M., Tyndall, G., et al.: A global simulation of tropospheric ozone and related tracers: Description and evaluation of MOZART, version 2, J. Geophys. Res, 108, 4784, 2003.

Horowitz, L. W., Fiore, A. M., Milly, G. P., et al.: Observational constraints on the chemistry of isoprene nitrates over the eastern United States, J. Geophys. Res., 112, D12S08, doi:10.1029/2006JD007747, 2007. 9873
Jacob, D. J., Logan, J. A., Gardner, G. M., Yevich, R. M., Spivakovsky, C. M., Wofsy, S. C., Sillman, S., and Prather, M. J.: Factors regulating ozone over the United-States and its export to the global atmosphere, J. Geophys. Res., 98, 14 817–14 826, 1993. 9878
Koch, D., Jacob, D., Tegen, I., Rind, D., and Chin, M.: Tropospheric sulfur simulation and sulfate direct radiative forcing in the Goddard Institute for Space Studies general circulation model, J. Geophys. Res., 104, 23 799–23 822, 1999. 9872
Liao, H., Adams, P. J., Chung, S. H., Seinfeld, J. H., Mickley, L. J., and Jacob, D. J.: Interactions between tropospheric chemistry and aerosols in a unifiegeneral circulation model, J. Geophys. Res., 108, 4001, doi:10.1029/2001JD001260, 2003. 9871, 9872, 9873
Liao, H., Seinfeld, J. H., Adams, P. J., and Mickley, L. J.: Global radiative forcing of coupled tropospheric ozone and aerosols in a unified general circulation model, J. Geophys. Res., 109, D24204, doi:10.1029/2003JD004456, 2004. 9871, 9872, 9873
Liao, H., Chen, W.-T., and Seinfeld, J. H.: Role of climate change in global predictions of future tropospheric ozone and aerosols, J. Geophys. Res., 111, D12304, doi:10.1029/2005JD006852, 2006. 9869, 9870
Logan, J. A.: An analysis of ozonesonde data for the lower stratosphere: Recommendations for testing models, J. Geophys. Res., 104, 16 151–16 170, 1999. 9872
Mickley, L. J., Murti, P. P., Jacob, D. J., Logan, J. A., Koch, D. M., and Rind, D.: Radiative forcing from tropospheric ozone calculated with a unified chemistry-climate model, J. Geophys. Res., 104, 30 153–30 172, 1999. 9871, 9872
Mickley, L. J., Jacob, D. J., and Field, B. D.: Effects of future climate change on regional air pollution episodes in the United States, Geophys. Res. Lett., 31, L24103, doi:10.1029/2004GL021216, 2004. 9870, 9876, 9877
Murazaki, K. and Hess, P.: How does climate change contribute to surface ozone change over the United States?, J. Geophys. Res., 111, D05301, doi:10.1029/2005JD005873, 2006. 9870, 9876
Racherla, P. N. and Adams, P. J.: Sensitivity of Global Tropospheric Ozone and Fine Particulate Matter Concentrations to Climate Change, J. Geophys. Res., 111, D24103, doi:10.1029/2005JD006939, 2006. 9869
Rind, D. and Lerner, J.: Use of on-line tracers as a diagnostic tool in general circulation model

development .1. Horizontal and vertical transport in the troposphere, J. Geophys. Res., 101, 12 667–12 683, 1996. 9871

Rind, D., Lerner, J., Shah, K., and Suozzo, R.: Use of on-line tracers as a diagnostic tool in general circulation model development 2. Transport between the troposphere and stratosphere, J. Geophys. Res., 104, 9151–9167, 1999. 9871

Robertson, A., Overpeck, J., Rind, D., Mosley-Thompson, E., Zielinski, G., Lean, J., Koch, D., Penner, J., Tegen, I., and Healy, R.: Hypothesized climate forcing time series for the last 500 years, J. Geophys. Res., 106, 14 783–14 803, 2001. 9875

Russell, G. L., Miller, J. R., and Rind, D.: A coupled atmosphere-ocean model for transient climate change studies, Atmosphere-Ocean, 33, 683–730, 1995. 9875

Sillman, S. and Samson, F. J.: Impact of temperature on oxidant photochemistry in urban, polluted rural and remote environments, J. Geophys. Res., 100, 11 497–11 508, 1995. 9869

Singh, H., OHara, D., Herlth, D., Sachse, W., Blake, D., Bradshaw, J., Kanakidou, M., and Crutzen, P.: Acetone in the atmosphere: Distribution, sources, and sinks, J. Geophys. Res, 99, 1805–1819, 1994. 9874

Stevenson, D. S., Johnson, C. E., Collins, W. J., Derwent, R. G., and Edwards, J. M.: Future estimates of tropospheric ozone radiative forcing and methane turnover the impact of climate change, Geophys. Res. Lett., 27, 2073–2076, 2000. 9869

Wang, Y. H., Jacob, D. J., and Logan, J. A.: Global simulation of tropospheric O_3-NO_x-hydrocarbon chemistry 1. Model formulation, J. Geophys. Res, 103, 10 713–10 725, 1998. 9872, 9874

Wesely, M. L.: Parameterization of surface resistances to gaseous dry deposition in regional-scale numerical-models, Atmos. Environ., 23, 1293–1304, 1989. 9872

Zeng, G. and Pyle, J. A.: Changes in tropospheric ozone between 2000 and 2100 modeled in a chemistry-climate model, Geophys. Res. Lett., 30, 1392, doi:10.1029/2002GL016708, 2003. 9869

Table 1. The ozone season (May through September) average value (μ) and standard deviation (σ) for key climate variables over the surface layer (984–934 hPa) of Southeast and Midtlantic (95–65° W and 24–40° N) and Northeast (95–65° W and 40–48° N) United States for the present climate (PC) and future climate (FC) simulations.

	PC Simulation		FC Simulation	
	μ	σ	μ	σ
Southeast and Midtlantic USA				
Air temperature (°C)	21.9	0.14	23.5	0.17
Total cloud cover (%)	59.4	1.39	58.2	1.33
Wind speed (m s^{-1})	4.5	0.25	4.7	0.27
Absolute humidity (10^{-4} kg H_2O/kg air)	126.0	1.69	137.0	1.82
Northeast USA				
Air temperature (°C)	15.9	0.14	17.6	0.18
Total cloud cover (%)	67.8	1.38	66.1	1.35
Wind speed (m s^{-1})	4.4	0.32	4.5	0.59
Absolute humidity (10^{-4} kg H_2O/kg air)	94.2	1.44	104.0	2.13

ACPD
7, 9867–9897, 2007

Table 2. Seasonal surface layer (984–934 hPa) ozone budget over the Southeast and Midatlantic United States (95–75° W and 28–40° N) for the present climate (PC) and future climate (FC) simulations. The budget presented here is for the odd oxygen (O_x) family defined as the sum of O_3, O, NO_2, 2 × NO_3, 3 × N_2O_5, HNO_4, HNO_3, and the peroxyacylnitrates.

	DJF		MAM		JJA		SON	
	PC	FC	PC	FC	PC	FC	PC	FC
Sources (Tg O_3/ 3 months)								
Chemical production	2.3	2.6	7.8	8.6	12.5	13.6	6.2	7.2
Sinks (Tg O_3/ 3 months)								
Dry deposition	1.5	1.6	4.6	4.6	5.5	5.6	3.2	3.5
Chemical loss	0.8	0.9	2.1	2.3	3.7	4.2	1.9	2.2
Net transport	0.0	0.1	1.1	1.7	3.3	3.8	1.1	1.5
Burden (Gg)	65.6	65.3	101.9	99.7	106.5	109.3	85.9	89.1
Lifetime (Hours)	61.7	55.2	28.9	25.7	18.8	17.8	30.4	27.0

Table 3. Seasonal variations of a number of factors controlling ozone chemical production over the surface layer (984–934 hPa) of the Southeast and Midatlantic United States (95–75° W and 28–40° N) for the present climate (PC) and future climate (FC) simulations. In this table, RO_2 includes peroxy radicals (lumped) formed from the oxidation of all non-methane VOCs with OH.

	DJF		MAM		JJA		SON	
	PC	FC	PC	FC	PC	FC	PC	FC
Isoprene emissions (Tg/3 months)	0.25	0.30	1.53	1.81	3.89	4.55	1.33	1.77
$NO+HO_2$ (Tg O_3/3 months)	1.32	1.45	4.16	4.50	5.96	6.28	3.20	3.63
$NO+CH_3O_2$ (Tg O_3/3 months)	0.25	0.28	0.81	0.88	1.24	1.32	0.62	0.71
$NO+RO_2$ (Tg O_3/3 months)	0.72	0.83	2.81	3.19	5.29	5.96	2.34	2.87
HO_2 (10^8 molecules cm^{-3})	0.23	0.28	0.89	1.03	1.69	1.87	0.70	0.92
RO_2 (10^4 molecules cm^{-3})	0.15	0.20	0.57	0.73	1.52	1.87	0.65	0.94
PAN (Gg)	2.96	2.69	3.30	2.99	2.32	2.18	2.73	2.53
NO_x (Gg)	9.85	9.70	5.83	5.81	4.18	4.09	7.50	7.07

Table 4. The average difference (future climate simulation minus present climate simulation) in the annual frequency of ozone episodes, and the ratio of the average difference to the standard error as a function of the number of simulation years for five select locations over the Southeast and Midatlantic United States.

	Average difference	Average difference : Standard error		
		1 years	5 years	10 years
95–90° W and 28–32° N	50	1.7	4.6	4.6
95–90° W and 32–36° N	36	1.2	3.9	3.4
85–80° W and 32–36° N	46	2.1	5.9	5.8
85–80° W and 36–40° N	25	2.0	4.6	4.3
80–75° W and 36–40° N	25	2.4	4.9	5.8

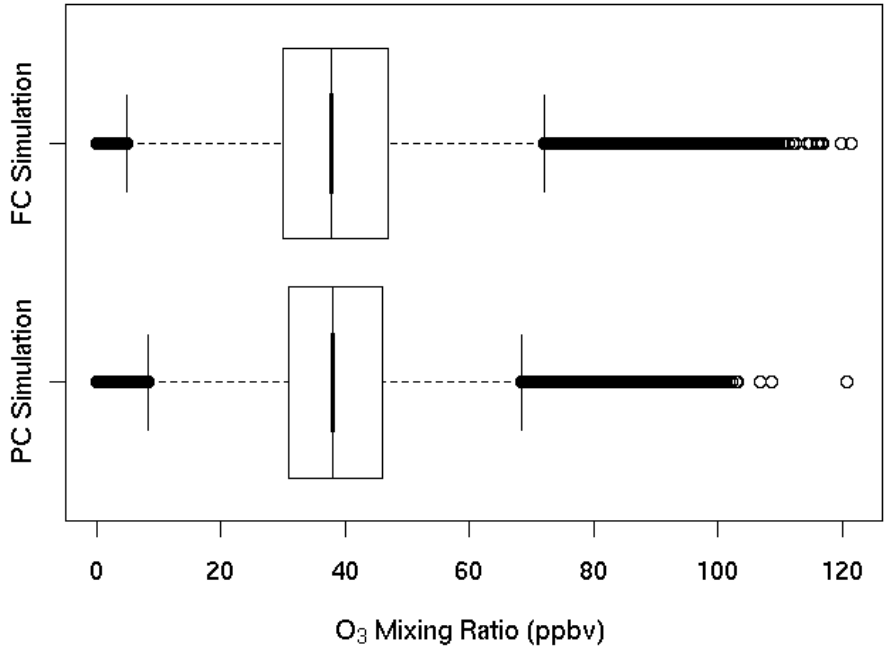

Fig. 1. Box and whisker plots of the 4-h average surface layer (984–934 hPa) ozone mixing ratios over the eastern United States (105–65° W and 24–48° N) for the present climate (PC) and future climate (FC) simulations. These data are not spatially averaged; they correspond to 4-h average surface ozone mixing ratios, 10 simulation years worth, saved over the eastern United States, corresponding to 38 model cells in total (pure ocean cells are excluded). The central box shows the data between the upper and lower quartiles (25th and 75th percentile), with the median represented by a vertical line; whiskers go out to the 5th and 95th percentiles of the data. Values beyond the 5th and 95th percentile are shown as individual data points.

ACPD
7, 9867–9897, 2007

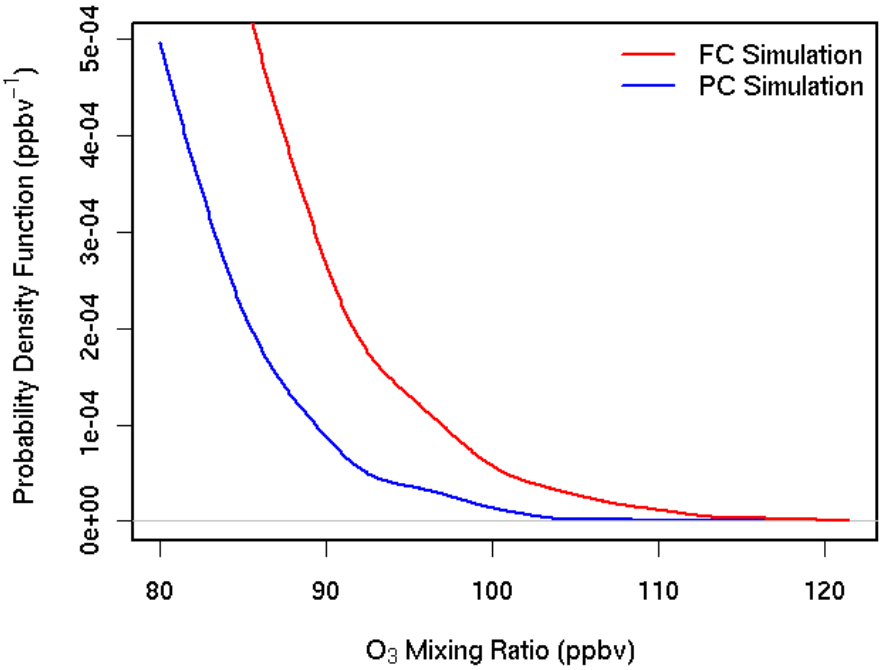

Fig. 2. Probability density function of the 4-h average surface layer (984–934 hPa) ozone mixing ratios over the eastern United States (105–65° W and 24–48° N) for the present climate (PC) and future climate (FC) simulations; only the upper tail (ozone mixing ratio ≥80 ppbv) of the distribution is shown here. These data are not spatially averaged; they correspond to 4-h average surface ozone mixing ratios, 10 simulation years worth, saved over the eastern United States, corresponding to 38 model cells in total (pure ocean cells are excluded).

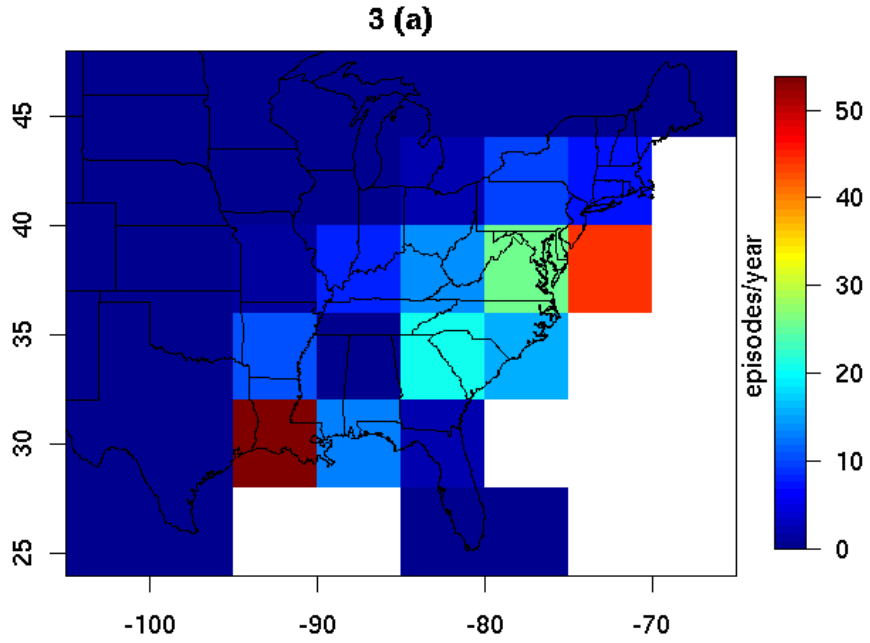

Fig. 3a. Average yearly frequency of ozone episodes (defined here as any occurrence in a grid cell of a 4-h average ozone mixing ratio greater than 80 ppbv) over the eastern United States corresponding to the present climate simulation.

ACPD
7, 9867–9897, 2007

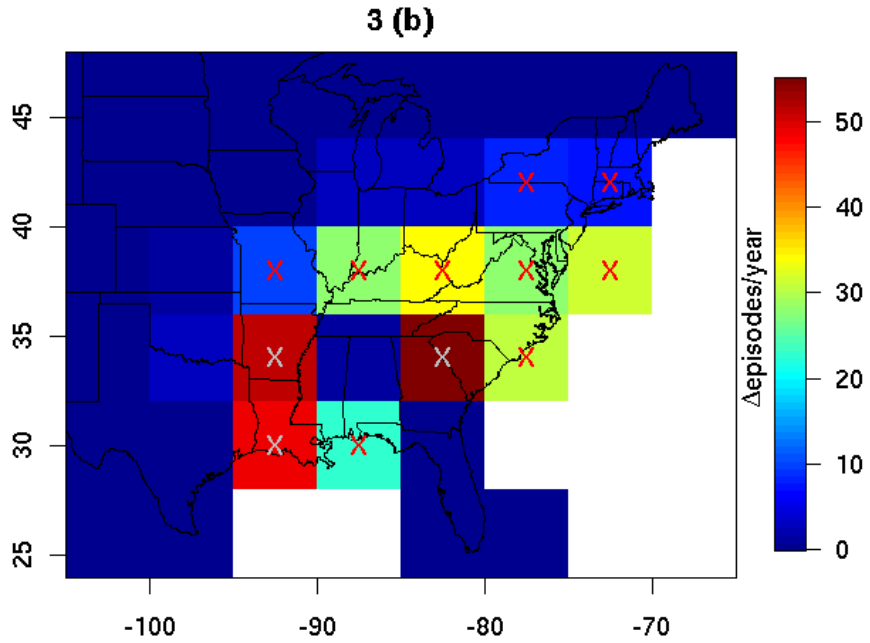

Fig. 3b. Differences (future climate simulation minus present climate simulation) in the average yearly frequency of ozone episodes over the eastern United States. Grid cells marked with an "X" have a statistically significant (p-value <0.05) difference in the yearly frequency of ozone episodes, which is determined using a Student's t test upon the 10-year distributions of the yearly frequency of ozone episodes in each model grid cell for the present and future climate simulations.

ACPD
7, 9867–9897, 2007

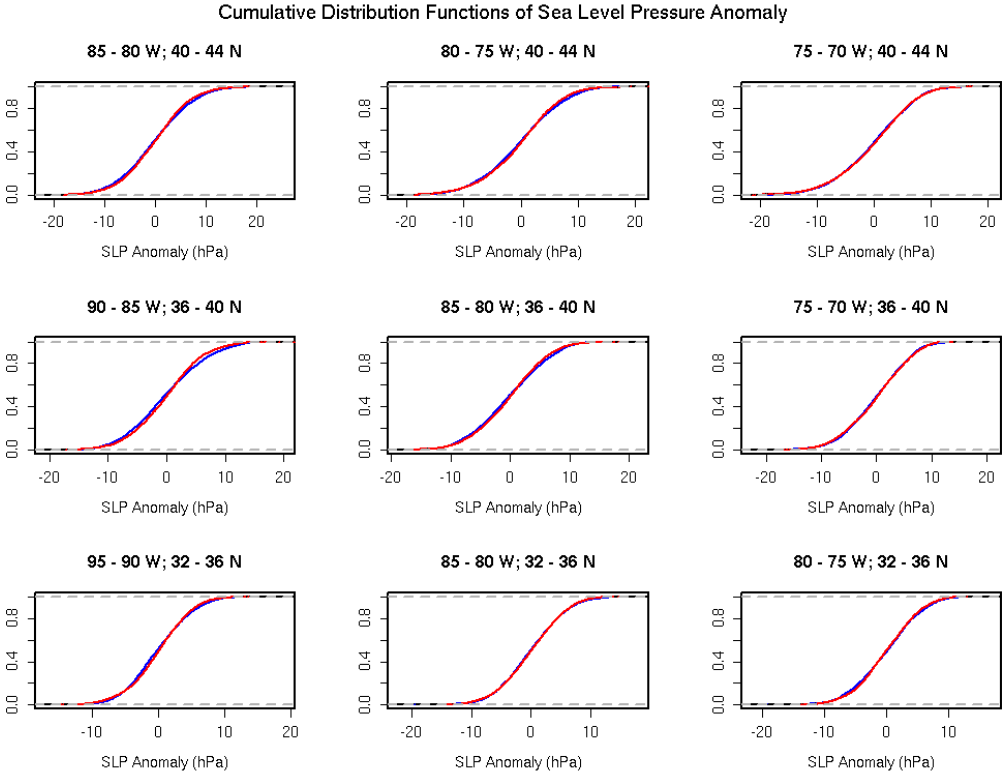

Fig. 4. Cumulative distribution functions (CDFs) of summertime (June/July/August) sea level pressure (SLP) anomaly (instantaneous value minus mean) for 9 different model grid cells spread over the Northeast (top row), midatlantic (middle row), and southeast (bottom row) United States for the present climate simulation (blue color line) and the future climate simulation (red color line). In each case, the y-axis represents the CDF and the x-axis the SLP anomaly (units of hPa).

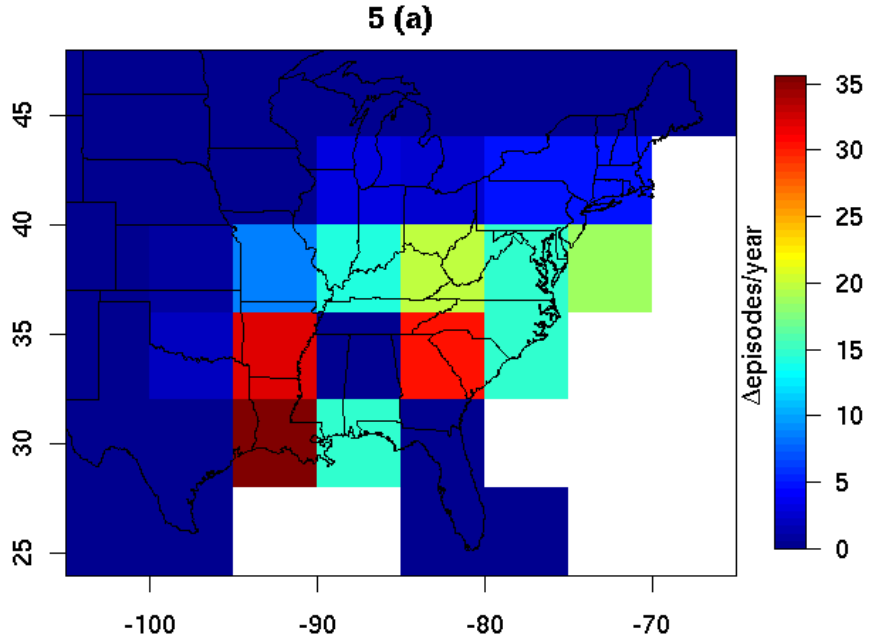

Fig. 5a. Differences (future climate simulation minus present climate simulation) in the summertime (June/July/August) frequency (5-year average) of ozone episodes (defined here as any occurrence in a grid cell of a 4-h average ozone mixing ratio greater than 80 ppbv) over the eastern United States.

ACPD
7, 9867–9897, 2007

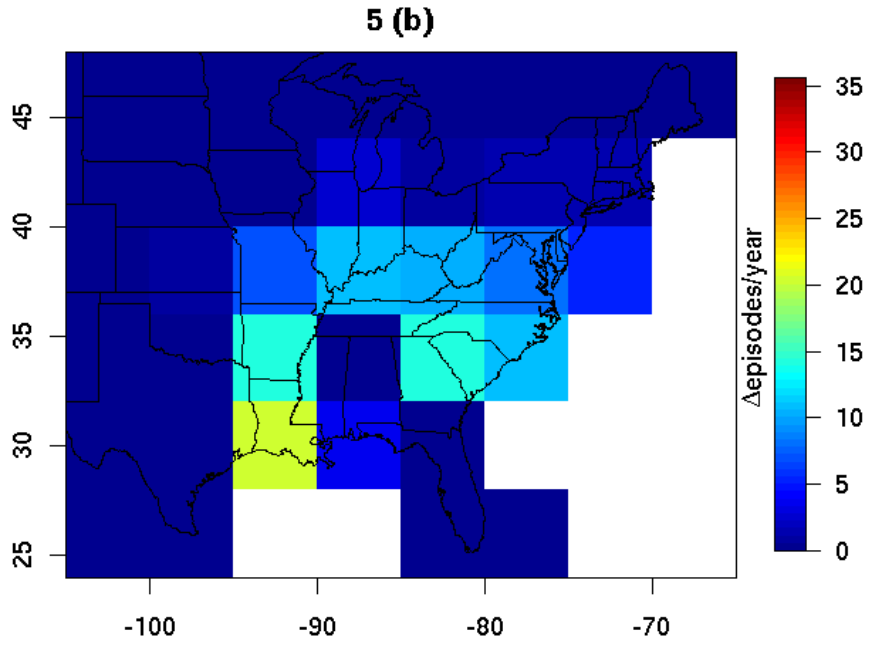

Fig. 5b. As in Fig. 5a but due to changes in isoprene emissions alone; see Sect. 3.2 for further details.

ACPD
7, 9867–9897, 2007

EGU

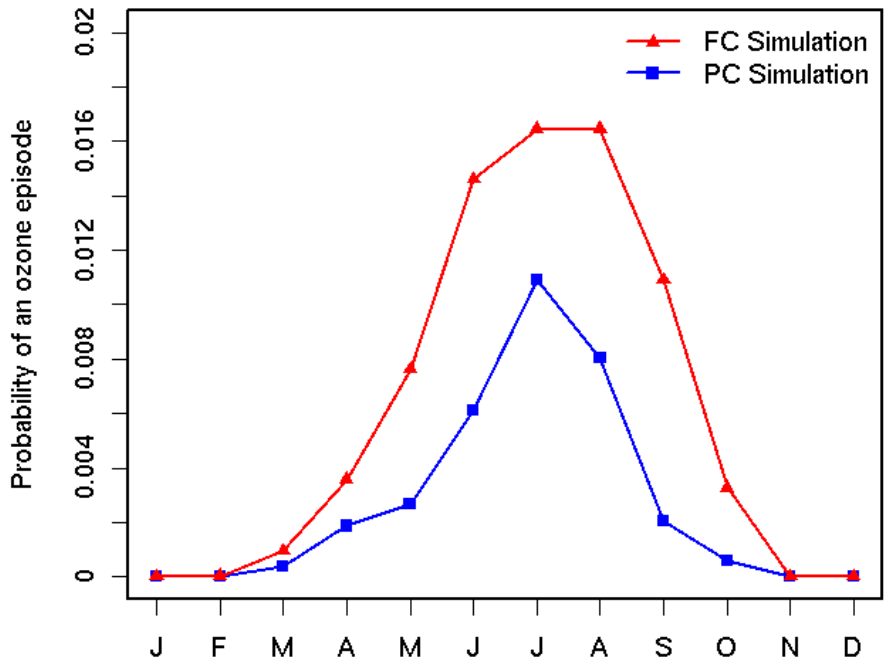

Fig. 6. The probability of an ozone episode (per model time step and grid cell) occuring over the eastern United States (105–65° W and 24–48° N) for the present climate (PC) and future climate (FC) simulations. Months J through D refer to months January through December. Monthly probabilities are calculated by normalizing the domain-wide monthly 4-h average ozone exceedances of 80 ppbv by the product of the number of grid cells (eastern United States) and simulation time steps for each month.